Kovove Mater. 52 2014 313–319
DOI: 10.4149/km_2014_5_313

Tribological behaviour and local mechanical properties of magnesium-alumina composites

S.-J. Huang[1], P.-C. Lin[2], B. Ballóková[3]*, P. Hvizdoš[3], M. Besterci[3]

[1] *National Taiwan University of Science and Technology, Department of Mechanical Engineering, 43, Sec. 4, Keelung Rd., 106 Taipei, Taiwan, R.O.C.*
[2] *National Chung Cheng University, Department of Mechanical Engineering, 168 University Rd., Ming-Hsiung, 621 Chia-Yi, Taiwan, R.O.C.*
[3] *Institute of Materials Research, Slovak Academy of Sciences, Watsonova 47, 040 01 Košice, Slovak Republic*

Received 16 August 2012, received in revised form 21 March 2014, accepted 21 March 2014

Abstract

Mechanical and wear properties of magnesium alloys based composite series with alumina dispersoid nanoparticles were studied. In order to achieve microstructures with very fine grains, the fabricated composites were further deformed and categorized as Severe Plastic Deformation (SPD). The as-received as well as the SPD treated states were characterized. Hardness and indentation modulus of elasticity of the materials were measured by instrumented indentation technique. Microstructure parameters were observed using transmission electron microscopy. Tribological properties were studied by ball-on-disk technique in dry sliding against steel balls at various temperatures from room temperature up to 573 K. Coefficient of friction and specific wear rates were evaluated. Worn surfaces were studied by scanning electron microscopy. Damage mechanisms were identified and their relationship with structural characteristics was inferred. Hardness of all materials was higher after SPD. Generally, the wear resistance of the magnesium based composites at high temperatures decreased.

K e y w o r d s: magnesium, alumina, ultra fine grains composite, severe plastic deformation, local mechanical properties, wear

1. Introduction

The performance of many metal alloys, usually in terms of strength and hardness, can be enhanced by the presence of extremely small and uniformed dispersed particles within the original phase matrix. These dispersoids can be introduced as insoluble particles in powder compaction (dispersion strengthening) or they can be formed during the solid state reaction as precipitates (precipitation or age strengthening). Such particles then effectively block dislocation motion which can lead to increased strength, stiffness, hardness, etc.

A way to achieve savings in industry is to make frequently used machinery lighter, often by using lightweight alloys but, if possible, without compromising their mechanical properties. Magnesium, as the lightest structural metal, is an attractive material for such structural applications, because of its high strength to weight ratio, which is better than that of aluminium and many other metals and alloys [1–3]. Magnesium alloys can be used in manufacturing automobile and aircraft wheels, automotive and aerospace parts, rollers, etc. [4, 5]. For many applications, particularly in the automotive industry, a demand for higher strength and also wear resistance has to be met. A potential method of achieving that is to make composites of Mg alloys and ceramic particles and/or fibres. For higher temperature applications, such as parts in thrust chambers, engine piston crown sides or the cylinder, good heat resistance is required. Kawamori and Machida [6] studied Mg alloys containing silicon carbide (SiC), which exhibits good thermal conductivity and high-temperature strength that can enhance high temperature properties of Mg-based composites. According to Semenov et al. [1] such com-

*Corresponding author: tel.: 00421 55 7922 411; fax: 00421 55 7922 408; e-mail address: bballokova@imr.saske.sk

Table 1. Chemical composition of AM60 (wt.%)

Elements	Al	Mn	Zn	Si	Fe	Cu	Ni	Mg
	5.8	0.32	0.22	0.1	0.005	0.01	0.002	Balance

posites with small amount of SiC can also exhibit higher strength. Francis and co-workers [7] studied magnesium strengthened materials obtained by mechanically admixed alumina nano particles with a hardness value equal to or higher than that of commercial Mg alloys and with increased flexural strength and work of fracture. S. Kumar et al. [8–9] investigated the effect of dual reinforced ceramic particles on high temperature tribological properties of aluminium composites. They found that the transition in the wear mode for all composites occurred after temperature 423 K. The decrease in coefficient of friction at this temperature was caused by the formation of the oxide layer on the sliding surface.

Besides dispersion strengthening, a convenient way to obtain desirable properties like higher strength and hardness can be achieved by creating very fine, submicron-grained microstructure [10] which, in essence, utilizes the Hall-Petch relationship. Such microstructure can be prepared by inducing severe plastic deformation – SPD [1, 11, 12]. Convenient techniques for doing that are the methods of cold working such as the Equal Channel Angular Pressing (ECAP) or Extrusion (ECAE) which by multiple pressings of material through the die create very fine grained nanostructure [13]. The materials prepared in this way are suitable for demanding parts of machines frequently exposed to intense friction and wear, such as washers, bearing liners, etc., where properties such as high strength and ductility, fatigue strength, wear resistance, etc., are required.

Thus, the magnesium based dispersion hardened composites can be further strengthened by SPD. However, information about the tribological behaviour of these materials is still scarce and the topic needs more profound study.

The aim of this work was to investigate the effect of refining of microstructure by SPD processes on local mechanical properties as well as on tribological behaviour and wear at room and elevated temperatures of magnesium ultra fine grained composites strengthened by alumina dispersoids.

2. Experimental materials

The matrix used in this work was a magnesium alloy AM60 with 5.8 % aluminium. Its chemical composition is shown in Table 1. Al_2O_3 particles with

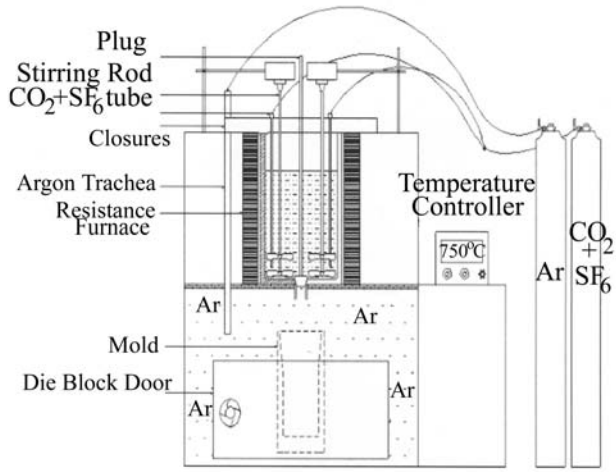

Fig. 1. Setup configuration.

weight fraction of 1, 2, and 5 % within metal matrix composites (MMCs) were used as the reinforcement phase. The commercially available Al_2O_3 powder with a particle diameter about 25 nm, purity of 99.8 %, was added into AM60 to form Mg-based metal-matrix composites.

The melt-stirring technique was used to fabricate the present Mg MMCs. Experimental setup is shown in Fig. 1. The AM60 was initially placed inside a graphite crucible and heated to 1023 K in a resistance-heated furnace. The molten alloy was stirred with a vane operated at 450 rpm for 10 min. Preheated Al_2O_3 particles were simultaneously added to the stirred alloy. Then the composite melt was finally poured into a metallic mould. The AM60 MMCs containing Al_2O_{3p} with different weight fraction of 1, 2, and 5 wt.% were prepared for further mechanical testing. The AM60 MMCs were homogenized at 673 K for 18 h and water quenched. These ingots were hot extruded by an extrusion ratio of 12 : 1 on a hydraulic press. Extrusion was carried out at 573 K. The preforms were held at 573 K for 90 min in a constant temperature furnace before extrusion. Colloidal graphite was used as a lubricant. Rods of 20 mm diameter were obtained after extrusion.

Billets of $11.4 \times 11.4 \times 95\,\mathrm{mm}^3$ were processed from the AM60 and AM60 MMCs' rods. The scheme of ECAP shown in Fig. 2 was carried out in a die with the die angle $\Phi = 120°$. The extrusion temperature was controlled within ± 5 K of the setting temperature, and the extrusion temperature was set at 573 K. During extrusion, the plunger speed was about $1\,\mathrm{mm\,s^{-1}}$. After each extrusion pass, the bullet was quenched into water. The billet was rotated counterclockwise about the exit extrusion axis by 90° between each pass, the so-called route Bc [12], and each billet was ECAPed 1, 2 and 4 times (Fig. 3).

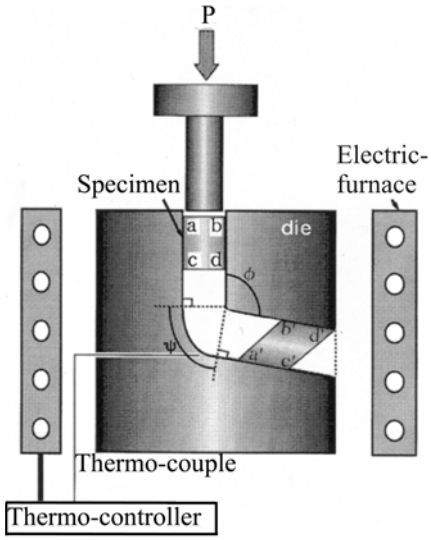

Fig. 2. The scheme of equal-channel angular pressing (ECAP).

3. Experimental methods

3.1. Microstructure study

In order to evaluate homogeneity of microstructure and to determine the average size of matrix grains, pores and inclusions, metallographic and EDX analyses were performed. Also, with the purpose to identify dispersed particles and secondary phases, TEM observations of thin foils and electron diffraction analysis were carried out.

3.2. Depth sensing indentation

Hardness and elastic modulus were measured using the depth sensing indentation (DSI) also called instrumented indentation technique. The method is based on controlled load and simultaneous extremely precise (< 0.1 nm) measurement of indenter penetration depth into the tested material.

The measurements were carried out on a nanoindentation tester TTX-NHT by CSM Instruments. Berkovich pyramid diamond tip was used in sinus mode loading of 5 Hz frequency and 5 mN load amplitude. Loads up to 100 mN were applied. The resulting load-penetration (P-h) curves were evaluated according to the analysis of Oliver and Pharr [15] and values of hardness and elastic modulus as functions of depth as well as elastic and plastic deformation energies were calculated. Up to 20 indentations were performed and the obtained data were statistically evaluated.

3.3. Wear testing

Wear testing was performed on a High Temperature Tribometer THT, by CSM Instruments, using a ball-on-disk technique. The sample was fixed on a turntable with adjustable rotational speed. The tangential force exerted on the holder was measured and from that the coefficient of friction (COF) was calculated and recorded as a function of distance/time/laps. The vertical position of the holder was measured in order to monitor the displacement due to material removed by wear. Steel balls (chromium steel 100Cr6 with hardness 62 HRC) with 6 mm diameter were used as friction partners. The loading of 1 N was applied using a dead weight system. The nominal wear track radius was 2 mm, the sliding speed was set to 5 cm s^{-1}, and the overall sliding distance was 100 m. Testing was done on air under dry conditions (humidity 40 % ± 5 %). Temperatures 293, 423 and 573 K were used. The heating was provided by an integrated furnace which reached the target temperature in the sample chamber in about 30 min and then during another 30 min it was allowed for the temperature to homogenize and stabilize. After the tests, both tribological partners (the steel ball and the sample)

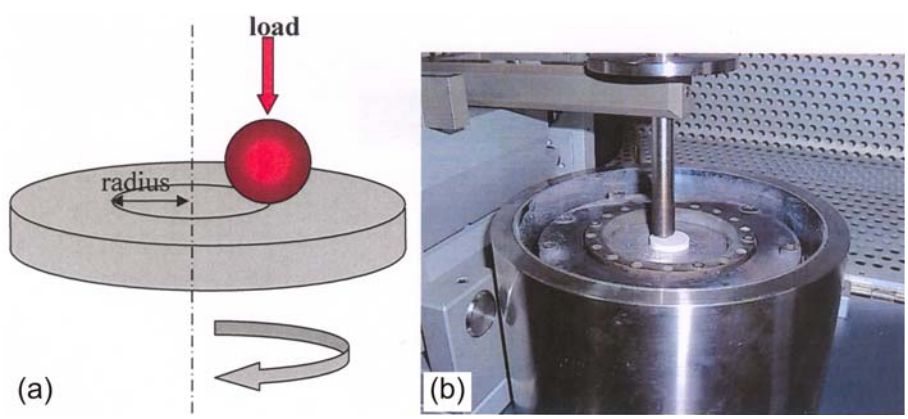

Fig. 3. Schematic illustration of ball-on-disk method (a) and experimental set-up of the test (b).

were observed using light microscopy. The depth and shape of the wear tracks were measured by a confocal microscope Plu neox 3D profiler by Sensofar. The average through cross section area was calculated and subsequently the volume of the removed material was estimated. The specific wear rates W were then expressed according to the standard ISO 20808, 2004 [14], as the volume loss V (mm^3) per distance L (m) and applied load F_p (N):

$$W = \frac{V}{LF_p}, \tag{1}$$

and used for comparison purposes.

4. Results and discussion

Microstructure parameters of the experimental materials, in particular the matrix grain size, average size of the dispersed particles and their distribution were evaluated. Microstructures of the experimental materials were heterogeneous with grain size of about 10 μm before extrusion and 8 μm after extrusion treatment. These values were similar for all systems, although there was slight tendency to smaller grains in materials with a higher volume fraction of Al_2O_3 particles. It was reported previously in [17, 18] that the heat deformation process of such materials, besides the formation of incorporated Al_2O_3 particles, also led to the creation of intermetallic compound $Mg_{17}Al_{12}$. Deformation took place through slip systems which mutually interacted by forming microcracks.

Transmission electron microscopy and selective electron diffraction confirmed presence of $Mg_{17}Al_{12}$ phase within the microstructure. The grains of this phase had a typical spherical morphology with size from 0.2–0.8 μm and they were coherent with the magnesium matrix, Fig. 4a. The diffraction pattern exhibited a body centered cubic structure with the lattice parameter $a = 1.0569$ nm, as depicted in Fig. 4b. Fine alumina particles were distributed randomly and showed a slight tendency of clustering.

Tables 2 and 3 show the results obtained from indentation testing. It is clear that extruded materials in all four cases have higher values of both hardness and modulus of elasticity. In the as-cast materials increasing alumina concentration led to lower values of hardness. In the case of the extruded materials the results of elasticity (Table 3) were in good agreement with the literature value of Young's modulus for magnesium, 45 GPa [19]. The lower values for the as-cast materials were mostly connected to the residual porosity which remained in the microstructure after initial compaction, but subsequently, during extrusion was reduced and effectively eliminated. The effect of alumina particles on hardness and elasticity is ambiguous. Adding 1 % Al_2O_3 led to an increase of both properties but further increase of alumina concentration led, in the as-cast materials, to lower values. This

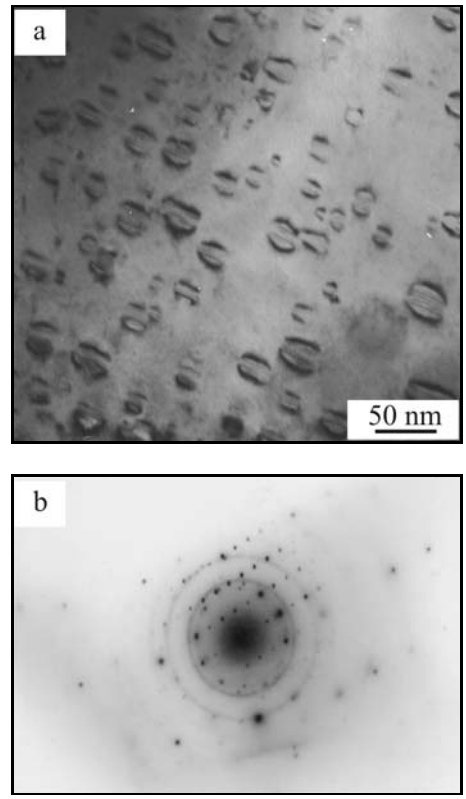

Fig. 4. Coherent $Mg_{17}Al_{12}$ particles observed in TEM using a thin foil (a) and their diffractogram (b).

Table 2. Hardness of experimental materials (MPa)

Material	As-cast	After ECAP
AM60	864 ± 37	949 ± 55
AM60 +1%Al_2O_3	1000 ± 45	1136 ± 38
AM60 + 2%Al_2O_3	912 ± 85	965 ± 48
AM60 + 5%Al_2O_3	812 ± 49	1109 ± 18

Table 3. Modulus of elasticity of experimental materials (GPa)

Material	As-cast	After ECAP
AM60	28.9 ± 4.8	37.0 ± 3.4
AM60 + 1%Al_2O_3	37.2 ± 4.5	42.8 ± 5.4
AM60 + 2%Al_2O_3	26.1 ± 5.6	39.0 ± 3.6
AM60 + 5%Al_2O_3	26.9 ± 5.2	44.5 ± 6.0

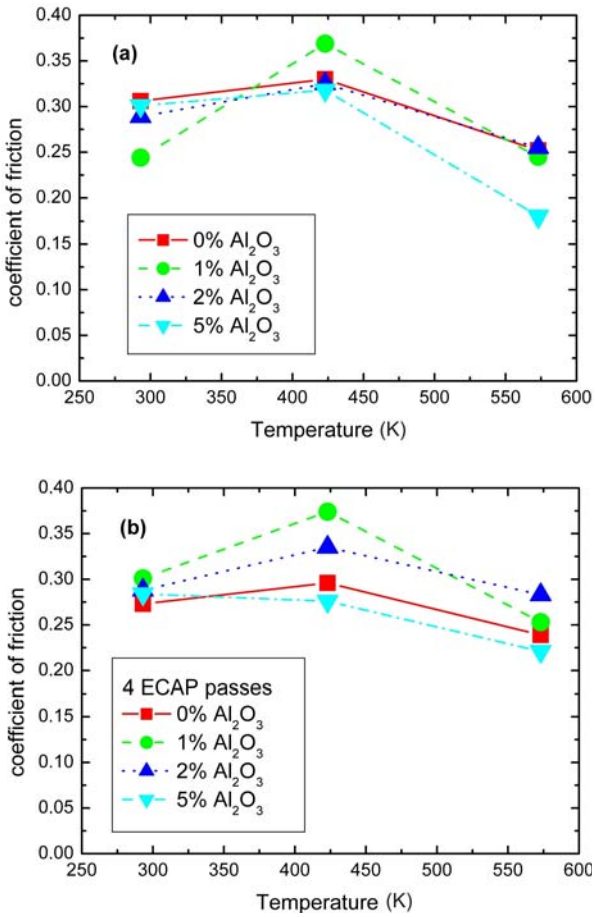

Fig. 5. Friction coefficient of the as-cast (a) and extruded (b) AM60-based materials as a function of temperature.

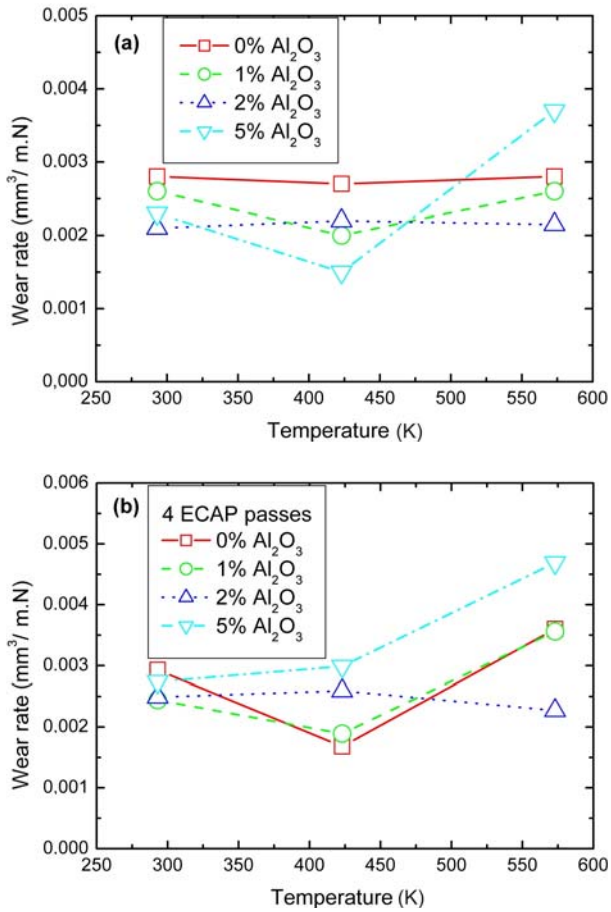

Fig. 6. Wear rates of the as-cast (a) and extruded (b) materials as a function of temperature.

is most probably connected with the tendency of alumina particles to clustering. Higher amount of dispersed particles then caused more porous and heterogeneous microstructure. However, the microstructure of AM60-5%Al_2O_3 became much more compact, and the hardness and elasticity modulus increased and reached similar values as in AM60-1%Al_2O_3.

Figure 5 shows average friction coefficient for all magnesium-based materials at temperatures 293, 423 and 573 K. At room temperature it is very similar, between 0.25 and 0.3. There is not much information about friction of magnesium based alloys in literature. For magnesium/magnesium dry contact the value is around 0.6 [20]. Naturally, as it is typical for self-mated friction, this is higher than that of magnesium/steel friction. Menezes [21] found COF for magnesium-steel dry wear to be between 0.35–0.45 depending on the surface texture. They studied its dependence on the surface finish and found that friction was decreasing with decreasing roughness (Ra) between 0.5 and 0.1 μm. The industrial data available at Applied Industrial Technologies [22] give for steel/Mg contact value of the COF = 0.25. These data are in a good agreement with our results, all of which were obtained for highly polished surfaces ($Ra < 0.05$ μm). As regards the effect of the temperature, Fig. 5a shows that there is a slight tendency to increase friction at first ($T = 423$ K). This can be connected to drop in humidity to zero. At even higher temperatures ($T = 573$ K), however, the coefficient of friction decreased again, probably due to softening of magnesium alloy and its easier surface deformation by the steel ball. The coefficient of friction decreased with increasing particle size of Al_2O_3 particles, particularly for volume fraction 5 % and temperatures 573 K. There was no significant difference in COF between the as-cast and extruded materials which means that there the chemical composition was the dominant factor.

Figures 6a,b show the plots of wear rate vs. testing temperature. Again, one can observe a slight decreasing tendency in the wear rate at 423 K when compared to the room temperature but it is not consistent for as-cast 2 % MMC, ECAPed 2 % MMC and ECAPed 5 % MMC. With further increase of temperature the wear rate again increased which is in agree-

ment with the suggestion that the tested materials at 573 K became softer and more deformation by the steel ball took place. At this temperature the wear rate increased the most for materials with 5 % Al_2O_3 secondary particles, while lower amounts of the secondary particles (1 and 2 %) had negligible effect on the change of the wear rate. The trend of wear rate decreasing firstly then increasing with increasing of temperature is consistent with results of S. Kumar et al. [8–9]. Furthermore, the character of the wear tracks suggested changes in the damage mechanisms. The decrease in wear rate at around 423 K was because of the formation of the oxide layer on the sliding surface. With further increase in temperature, the wear rate increased sharply. It is suggested that between 373 and 423 K formation of an oxide layer on the surface of ball protected the surface causing a decrease in wear rate. Above 423 K the transition from mild to severe wear occurred and matrix became more soft causing detachment of the formed oxide layer by delamination mechanism [23].

While the tracks at lower temperatures have a regular shape (Figs. 7a,b) with constant depth along the circumference, in the tracks made at 573 K a pattern of valleys and ridges started to form as shown in Fig. 7c. This suggests that besides abrasion, which is dominant at the lower two temperatures, at 573 K a combination of abrasion and adhesion occurred leading to so-called slip-stick phenomenon. In the beginning occasional sticking of the ball and sample and subsequent slipping led to formation of changes in the track depth, which then caused repetition of adhesive and abrasive wear [24] and resulted in forming an oscillating wear depth pattern, as it is schematically illustrated in Fig. 8.

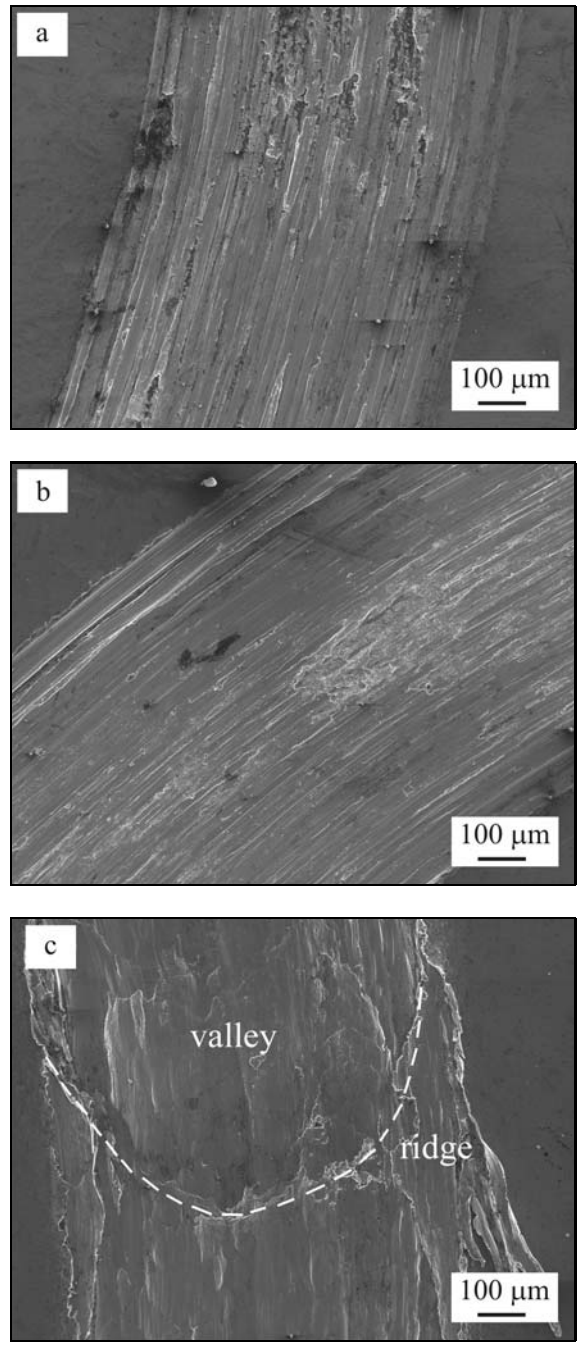

Fig. 7. Wear tracks in AM60 at room temperature (a), 423 K (b), and 573 K (c).

5. Conclusions

The difference between the as-cast and extruded Mg-Al_2O_3 materials is the variation in the microstructure where micro-sized grains and ultra fine grains were observed, respectively. Moreover, the as-cast materials also contain residual porosity which got eliminated after extrusion. Influence of volume fraction of the secondary Al_2O_3 phase on tribological characteristics is not significant. This follows from the relatively low amount of these particles (< 5 %) while the distribution of both types of particles, Al_2O_3 and intermetallic $Mg_{17}Al_{12}$, is heterogeneous. However, the effect of the deformation parameters on the local mechanical properties is manifested.

In summary, it has been shown that local mechanical properties as well as tribological behavior, are affected by lattice, physical parameters of phases within the composite systems. They are also affected by microstructure and substructure, which depend on the technology of compaction and densification (ECAP), above all by the matrix grain size and volume fractions and distribution of secondary phases (coherent, non-coherent, porosity).

Dominant wear mechanism is abrasion, at higher temperature, 573 K, also oscillation between abrasion and adhesion mechanisms starts to play an important role.

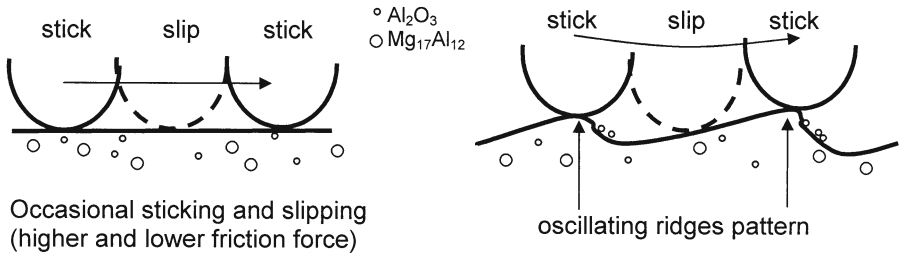

Fig. 8. Schematic illustration of slip-stick mechanism.

Acknowledgement

The work was financed by the project VEGA 2/0118/14.

References

[1] Semenov, V. I., Jeng, Y.-R., Huang, S.-J., Dao, Y.-Zh., Hwang, S.-J., Shuster, L. Sh., Chertovskikh, S. V., Lin, P.-Ch.: J. Friction and Wear, *30*, 2009, p. 194. doi:10.3103/S1068366609030088

[2] Harrington, W. C.: Mechanical Properties of Metallurgical Composites. New York, Marcel Dekker 1994.

[3] Kaczmar, J. W., Pietrzak, K., Wlisinski, W.: J. Mater Process Technol., *106*, 2000, p. 58. doi:10.1016/S0924-0136(00)00639-7

[4] Saravanan, R. A., Surppa, M. K.: Mater. Sci. Eng. A, *276*, 2000, p. 108. doi:10.1016/S0921-5093(99)00498-0

[5] Reddy, S. U., Srikanth, N., Gupta, M., Sinha, S. K.: Adv. Eng. Mater., *6*, 2004, p. 957. doi:10.1002/adem.200400105

[6] Kawamori, S., Machida, T.: Materials Transactions, *49*, 2008, p. 304. doi:10.2320/matertrans.P-MRA2007883

[7] Francis, E. D., Eswara Prasad, N., Ratnam, Ch., Sundra Kumar, P., Venkata Kumar, V.: Int. J. Adv. Sci. Technology, *27*, 2011, p. 35.

[8] Kumar, S., Poanwar, R. S., Pandey, O. P.: Metallurgical and Materials Transactions A, *44*, 2013, p. 1549.

[9] Kumar, S., Panwar, R. S., Pandey, O. P.: Ceramics International, *39*, 2013, p. 6333. doi:10.1016/j.ceramint.2013.01.059

[10] Gleiter, H.: Nanostructured Materials, *1*, 1992, p. 1. doi:10.1016/0965-9773(92)90045-Y

[11] Valiev, R. Z., Krasilnikov, N. A., Tsenev, N. K.: Mater. Science Eng. A, *137*, 1991, p. 35. doi:10.1016/0921-5093(91)90316-F

[12] Valiev, R. Z., Estrin, Y., Horita, Z., Langdon, T. G., Zehetbauer, M. J., Zhu, Y. T.: Journal of Metals, *58*, 2006, p. 33.

[13] Kunz, L., Lukáš, P., Svoboda, M.: Mater. Science Eng. A, *424*, 2006, p. 97. doi:10.1016/j.msea.2006.02.029

[14] Ding, S. X., Lee, W. T., Chang, C. P., Chang, L. W., Kao, P. W.: Scripta Materialia, *59*, 2008, p. 1006. doi:10.1016/j.scriptamat.2008.07.007

[15] Oliver, W. C., Pharr, G. M.: J. Mater. Res., *7*, 1992, p. 1564. doi:10.1557/JMR.1992.1564

[16] ISO 20808:2004(E): Fine Ceramics – Determination of Friction and Wear Characteristics of Monolithic Ceramics by Ball-on-Disc Method, 2004.

[17] El-Morsy, A., Ismail, A., Waly, M.: Mat. Sci. Eng. A, *486*, 2008, p. 528. doi:10.1016/j.msea.2007.09.044

[18] Lin, P.-C., Huang, S. J., Hong, P. S.: Acta Metallurgica Slovaca, *16*, 2010, p. 237.

[19] Engineering Toolbox. http://www.engineeringtoolbox.com/young-modulus-d_417.html. Retrieved 2013-03-18.

[20] Engineering Toolbox. http://www.engineeringtoolbox.com/friction-coefficients-d_778.html. Retrieved 2013-03-18.

[21] Menez, P. L., Kishore, A., Kailas, S. V.: Wear, *261*, 2006, p. 578. doi:10.1016/j.wear.2006.01.001

[22] Applied Industrial Technologies. http://web.applied.com/assets/attachments/492ACC9E-E5C2-2D43-0B8CCDA72ACE3361.pdf. Retrieved 2013-03-25.

[23] Sharma, V., Kumar, S., Panwar, R. S., Pandey, O. P.: Journal of Materials Science, *47*, 2012, p. 6633. doi:10.1007/s10853-012-6599-4

[24] Kondoh, K., Umeda, J., Kawabata, K., Seki, Y., Kawamura, Y.: Transactions of JWRI, *37*, 2008, p. 45.